Journal of Saudi Chemical Society (2017) **21**, 270–276

King Saud University

Journal of Saudi Chemical Society

www.ksu.edu.sa
www.sciencedirect.com

ORIGINAL ARTICLE

Interaction of CNCl molecule and single-walled AlN nanotubes using DFT and TD-DFT calculations

Alireza Soltani [a,*], Ahmad Sousaraei [a], Mehdi Mirarab [a], Hanzaleh Balakheyli [b]

[a] *Young Researchers and Elite Club, Gorgan Branch, Islamic Azad University, Gorgan, Iran*
[b] *Joints, Bones and Connective Tissue Research Center, Golestan University of Medical Science, Gorgan, Iran*

Received 18 February 2015; revised 23 May 2015; accepted 18 June 2015
Available online 9 July 2015

KEYWORDS

AlN nanotubes;
CNCl;
Electronic properties;
TD-DFT

Abstract Density functional theory (DFT) calculations are used to study the influence of cyanogen chloride (CNCl) adsorption over the geometrical and electronic properties of single-walled (5, 0), (8, 0), and (10, 0) AlN nanotubes as an adsorbent for adsorbate. It has been found that, the CNCl can be adsorbed on (5, 0), (8, 0), and (10, 0) AlN nanotubes with the energy values of −0.645, −0.493, −0.470 eV, respectively. In addition, the effect of nanotube diameter over the charge transfer between the molecule and nanotube has been studied. Based on the DOS plots, interaction of CNCl over AlN nanotubes has slightly changed the electronic properties of the nanotubes, being insensitive to the adsorption of the CNCl molecule.

1. Introduction

Cyanogen chloride or CNCl gas has high toxicity in animal and human bodies which leads to respiratory failure and blockage of the cellular energy metabolism. CNCl is a colorless and odorless gas which has been used in chemical warfare applications. Research has established that CNCl is particularly drastic for its capability of penetrating the filters in gas masks [1–4]. As an important member of group III-nitrides, AlN is characterized by its unique properties such as superior mechanical strength, high thermal conductivity, high melting point, high resistance to chemicals, and reliable dielectric properties [5–8], which make it extensively used in the electronics and optoelectronics industry. Experimentally, in 2002, AlN nanostructures have been successfully synthesized using a highly non-equilibrium dc–ac plasma technique with the diameter ranging from 30 to 80 nm, in gram quantities [9]. However, hexagonal AlN nanotubes have been experimentally synthesized in 2003 [10]. They are semiconductors with a wide band gap, indicating good dielectric properties, with high melting point, excellent thermal conductivity, and low thermal expansion coefficient [11], thereby are widely applied in today's electronic industry. For AlNNTs, typically when the tube diameter reduces it was followed by an energy gap decrease,

* Corresponding author. Tel.: +98 938 4544921.
E-mail address: Alireza.soltani46@yahoo.com (A. Soltani).
Peer review under responsibility of King Saud University.

ELSEVIER Production and hosting by Elsevier

http://dx.doi.org/10.1016/j.jscs.2015.06.006
1319-6103

owing to an increasing hybridization between the π and σ levels and a downshift of the π^* level as the curvature is increased [12]. Vurgaftman and Meyer [13] reported the band gap of hexagonal AlN with an experimental value of 6.2 eV. Mahdavifar and Haghbayan reported that the AlN nanotube has an energy gap of about 4.88 by the MPW1PW91 method and 2.76 eV by the PBE method using DFT calculations [14]. In recent years, vast researches have been performed upon the reliable chemical gas sensors for the detection of many toxic gas molecules containing HF, HCOH, OCN^-, N_2O, SCN^-, and H_2S with AlN nanostructures [15–20]. Jiao et al. indicated the adsorptions of CO_2 and N_2 over AlN nanotubes using two different functionals [21]. Recently, Liu and co-workers reported the adsorption of H_2, H_2O, O_2, and N_2 molecules on the N and Al-rich-ended (10, 0) and (6, 6) AlN nanotubes using DFT calculations [22]. The objective of this report was the adsorption of the CNCl molecule on (5, 0), (8, 0), and (10, 0) AlN nanotubes using DFT calculations.

2. Computational methods

The present studies are based on the adsorption of the CNCl molecule over the pristine (5, 0), (8, 0), and (10, 0) AlNNTs using density functional theory (DFT) and time-dependent density functional theory (TD-DFT) calculations. All the geometrical relaxations and binding energy computations have been carried out using the GAMESS suite of program [23] at the level of density functional theory (DFT) by the Becke-3-Lee–Yang–Parr (B3LYP) method with 6-31G** basis set [24–28]. All the stable structures were fully optimized with optimization criteria (Max. force = 0.00045, RMS force = 0.0003, max. displacement = 0.0018, and RMS displacement = 0.0012). All the nanotubes were built using the Nanotube Modeler [29] with appropriate initial assumption of the Al–N bond obtained from the literature. We also defined the adsorption energy (E_{ads}) of a CNCl molecule over the AlNNT as:

$$E_{ads} = E_{cluster-adsorbate} - (E_{cluster} + E_{adsorbate}) + E_{BSSE} \quad (1)$$

where $E_{adsorbent-adsorbate}$ are the total energies of the gas molecule on the outer wall of AlNNT. $E_{adsorbent}$ is the total energy of the pure AlNNT. $E_{adsorbate}$ is the total energy of the CNCl molecule. Basis set superposition error (BSSE) for the adsorption energies was corrected using the counterpoise method. Mulliken population charge analysis (MPA), and total density of states (TDOS) analyses were performed using the B3LYP method with 6-31G** basis set. Quantum molecular descriptors for AlN nanotubes were determined as follows:

$$\mu = -(I + A)/2 \quad (2)$$

$$\chi = -\mu \quad (3)$$

$$\eta = (I - A)/2 \quad (4)$$

$$S = 1/2\eta \quad (5)$$

$$\omega = (\mu^2/2\eta) \quad (6)$$

Electronegativity (χ) is defined as the negative of chemical potential (μ), as follows: $\chi = -\mu$. Furthermore, the global hardness (η) can be determined using the equation 5. I ($-E_{HOMO}$) is the ionization potential and A ($-E_{LUMO}$) is the electron affinity of the molecule. ω and S are the electrophilicity index and global softness of the systems.

3. Results and discussion

3.1. Cyanogen chloride adsorption

In Fig. 1, we have considered three kinds of AlN nanotubes, including *zigzag* (5, 0) or $Al_{30}N_{30}H_{10}$, (8, 0) or $Al_{48}N_{48}H_{16}$, and (10, 0) or $Al_{60}N_{60}H_{20}$ that are generated from a H-saturated tube through the respective breaking of the Al–H and N–H bonds. The charge density analysis using MPA analysis represents that the Al atoms of (5, 0), (8, 0), and (10, 0) AlN nanotubes are positively charged with values of 0.853, 0.855, and 0.860e and the N atoms are negatively charged with the same quantity. Accordingly, the electron deficient aluminum atoms are as a Lewis acid, while the electron-rich nitrogen atoms are as a Lewis base. Then, we considered the adsorption of Cyanogen chloride toward an Al site of (5, 0), (8, 0), and (10, 0) AlN nanotubes. When one Cyanogen chloride is adsorbed toward the Al site of (5, 0), (8, 0), and (10, 0) AlN nanotubes, the length of Al–N bonds in these nanotubes is increased from 1.8113, 1.8109, and 1.8107 in the pristine nanotubes to 1.8358, 1.8354, 1.8348 , respectively. Jiao et al. [30] have shown that the length of the Al–N bond in LDA and GGA methods is about 1.797 and 1.816 , respectively. Lim and Lin [31] indicated that the length of the Al–N bond in (8, 0) AlN nanotube is 1.830 . This result is close to the bond length of AlN nanotube reported by our calculations. As shown in Table 1, the estimated adsorption energies for a single CNCl molecule close to the Al sites of (5, 0), (8, 0), and (10, 0) AlN nanotubes are about −0.645, −0.493, −0.470 eV, implying a chemical bond in the interaction. The distances between the CNCl molecule and (5, 0), (8, 0), and (10, 0) AlN nanotubes are 2.075, 2.109, and 2.120 , respectively. The bond length (d_{C-N}) of the CNCl molecule attached to (5, 0), (8, 0), and (10, 0) AlN nanotubes is calculated to be 1.1564, 1.1571, and 1.1573 and that in the isolated CNCl molecule is 1.1631 , respectively. Therefore, the value of the bond length change, owing to the adsorption of the CNCl molecule, is almost large. Recently, Soltani and co-workers reported the adsorption of N_2O molecule on the outer wall of (6, 0) and (4, 4) AlN nanotubes using DFT calculations [18]. They showed that the adsorption of N_2O over (6, 0) and (4, 4) AlN nanotubes for Al site in N and O sides is calculated to be −0.28 and −0.24 eV, respectively. Noei and co-workers [15] revealed that the HF adsorption toward (5, 0) zigzag AlN nanotube is about 3.04 eV. To better understand the adsorption properties of cyanogen chloride attached to the AlN nanotube, the Mulliken population analysis data were studied. It was found that charge transfer from the CNCl molecule to (5, 0), (8, 0), and (10, 0) AlN nanotubes is about 0.189, 0.163, and 0.154 electrons, respectively. A lone pair of electrons over the N atom of CNCl makes it an electron rich molecule and therefore, it functions as a donor in this form and loses electrons. The charge transfer procedure combining with a more negative E_{ads} value could be a sign of a strong electrostatic interaction. The work function (Φ) is determined as the minimum energy that is required to remove an electron from the HOMO or the highest occupied energy

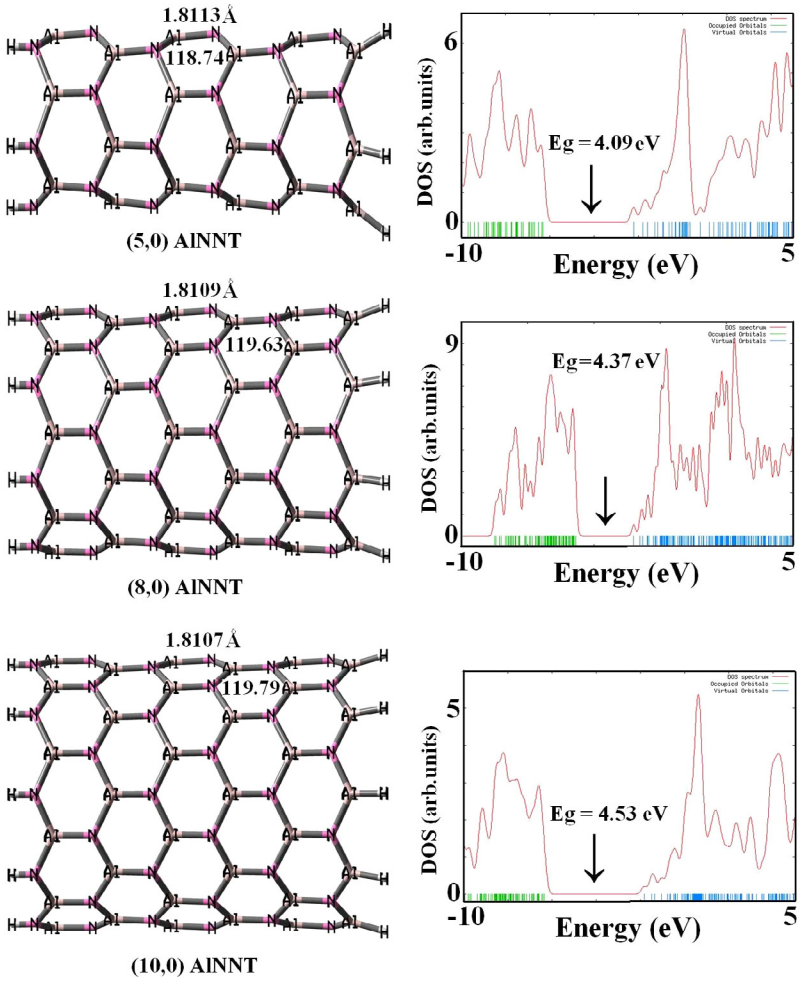

Figure 1 Optimized models of (5, 0), (8, 0) and (10, 0) AlNNTs and their density of state plots.

Table 1 Structure and electronic properties of CNCl interacted with AlN nanotubes.

Property	CNCl	(5, 0) AlN	(8, 0) AlN	(10, 0) AlN	CNCl/(5, 0) AlN	CNCl/(8, 0) AlN	CNCl/(10, 0) AlN
Al–N	–	1.811	1.811	1.8.11	1.836	1.835	1.835
Al–N–Al	–	116.19	118.48	118.99	118.45	120.00	120.29
N–Al–N	–	118.74	119.65	119.77	115.72	116.89	117.08
C–N	1.163	–	–	–	1.156	1.157	1.157
C–Cl	1.645	–	–	–	1.629	1.631	1.631
E_{HOMO} (eV)	−9.15	−6.31	−6.37	−6.36	−6.03	−6.13	−6.13
E_{LUMO} (eV)	−0.41	−2.22	−2.00	−1.83	−1.96	−1.82	−1.70
E_g (eV)	8.74	4.09	4.37	4.53	4.07	4.31	4.43
ΔE_g (%)	–	–	–	–	−0.49	−1.37	−2.21
Φ (eV)	4.37	2.05	2.19	2.27	2.04	2.16	2.22
ΔΦ (eV)	–	–	–	–	−0.48	−1.37	−2.20
DM (Debye)	2.67	12.34	15.90	18.61	15.47	18.32	20.57
E_{ad} (eV)	–	–	–	–	−0.645	−0.493	−0.470
E_F (eV)	−4.78	−4.27	−4.19	−4.10	−4.00	−3.98	−3.92
I (eV)	9.15	6.31	6.37	6.36	6.03	6.13	6.13
A (eV)	0.41	2.22	2.00	1.83	1.96	1.82	1.70
η (eV)	4.37	2.05	2.19	2.27	2.04	2.16	2.22
μ (eV)	−4.78	−4.27	−4.19	−4.10	−4.00	−3.98	−3.92
S (eV^{-1})	0.11	0.24	0.23	0.22	0.25	0.23	0.23
ω (eV)	2.61	4.45	4.01	3.70	3.92	3.67	3.46

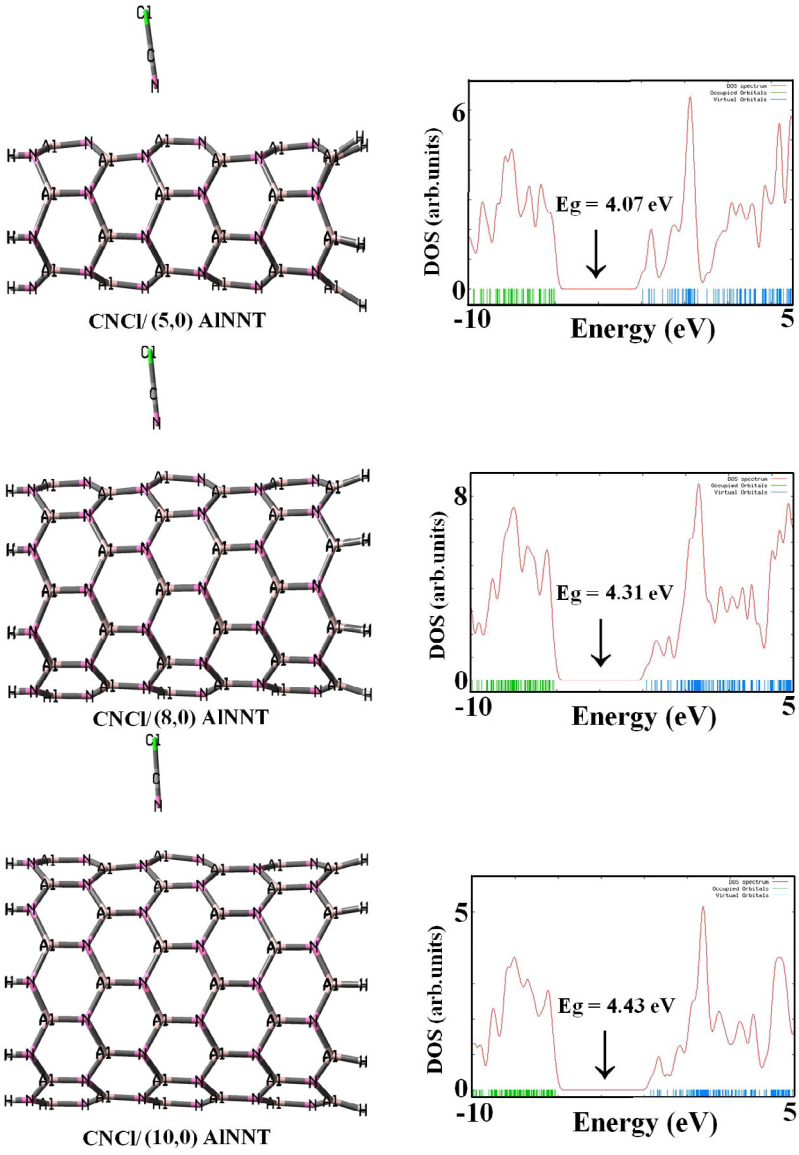

Figure 2 Optimized models of CNCl attached to (5, 0), (8, 0) and (10, 0) AlNNTs and their density of state plots.

Table 2 Selected excitation energies (E, nm), oscillator strength (f), and relative orbital contributions of calculated using the B3LYP method.

Methods	Wavelength (nm)	Oscillator strength (f)	Assignment
CNCl/(5, 0) AlN	375.66	0.0002	H → L (94%)
	353.53	0.0007	H-1 → L (90%), H-3 → L (2%), H-3 → L + 2 (2%)
	341.83	0.0002	H-3 → L (73%), H-4 → L (7%), H-4 → L + 2 (8%)
CNCl/(8, 0) AlN	327.46	0.0002	H → L (91%)
	323.92	0.0003	H-1 → L (90%)
CNCl/(10, 0) AlN	315.12	0.0001	H → L (76%), H → L + 1 (10%), H → L + 5 (4%)
	311.01	0.0002	H-1 → L (78%), H-1 → L + 1 (3%), H-1 → L + 5 (5%)

level in the solid to the vacuum. It can be calculated from the energy difference between the potential in the vacuum region and the Fermi level energy. However, the emitted electron current densities in vacuum are theoretically described by the following classical equation:

$$j = AT^2 \exp(-\Phi/kT) \leftarrow$$

where A is called the Richardson constant (A/m^2), T is the temperature (K) and Φ (eV) is the material's work function. Work function values were calculated using the following equation:

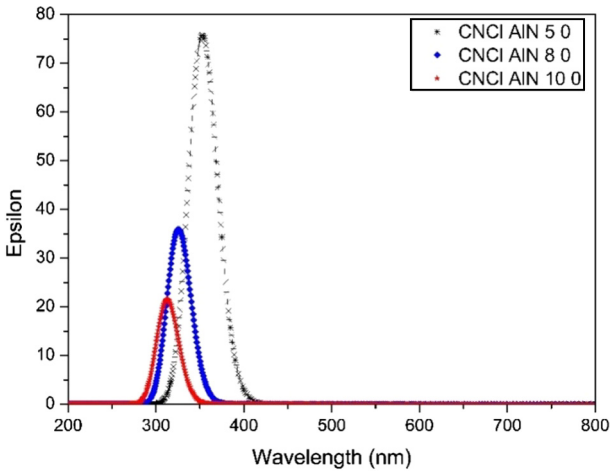

Figure 3 UV–Vis spectra of the CNCl molecule upon AlN nanotubes.

$$\Phi = E_{inf} - E_F$$

where E_{inf} is the electrostatic potential at infinity and E_F is the Fermi level energy. The electrostatic potential at infinity is assumed to be zero. The values of Φ for (5, 0), (8, 0), and (10, 0) AlN nanotubes are calculated to be 2.05, 2.19, and 2.27 eV, respectively. After the adsorption of the CNCl molecule, the Φ values are slightly reduced to 2.00, 2.16, and 2.22 eV, respectively. Therefore, the interaction between the CNCl molecule and the AlN nanotube leads to a reduction in work function. A negative work function change (ΔΦ) may enhance from a donation of charge from the CNCl to the surfaces of the tube which correlates with an increase in the tube conductance upon exposure to the target adsorbate. To understand the electronic properties of AlN nanotubes over reacting with the CNCl molecule, we performed electronic structure analysis by calculating total density of state (TDOS) plots for these configurations, as can be seen in Fig. 1. The TDOS plots clearly indicate that the energy gaps of (5, 0), (8, 0), and (10, 0) AlN nanotubes are about 4.09, 4.37, and 4.53 eV, respectively. Beheshtian et al. indicated that the energy gap of (5, 0) AlN nanotube is calculated to be 4.11 eV at B3LYP/6-31G* level of theory [32]. The energy gaps of (5, 0), (8, 0), and (10, 0) AlN nanotubes during the interaction process with the CNCl molecule are slightly changed to the values of 4.07, 4.31, and 4.43 eV, respectively (see Fig. 2). These calculations result in an increase of the tube diameter from (5, 0) to (10, 0) AlN nanotube, leading to enhancement in the electronic properties during the adsorption process. The Fermi level (E_F) after the adsorption of CNCl over (5, 0), (8, 0), and (10, 0) AlN nanotubes is slightly reduced as the changes of E_F for these systems are about 6.33%, 5.02%, 4.40%, respectively. Besides, the change of E_F slightly depends on the types of AlN nanotubes. Accordingly, we considered that the pure AlN nanotube is slightly sensitive to the presence of the CNCl molecule. For future study over the adsorption behavior of the CNCl molecule over the provided adsorbents, we prepared the quantum molecular descriptors of these systems. The global hardness of the pure (5, 0) AlN, (8, 0) AlN, and (10, 0) AlN nanotubes is slightly changed from 2.05, 2.19, and 2.27 eV to 2.04, 2.16, and 2.22 eV for the CNCl-adsorbents systems, respectively. For the CNCl/(10, 0) AlNNT

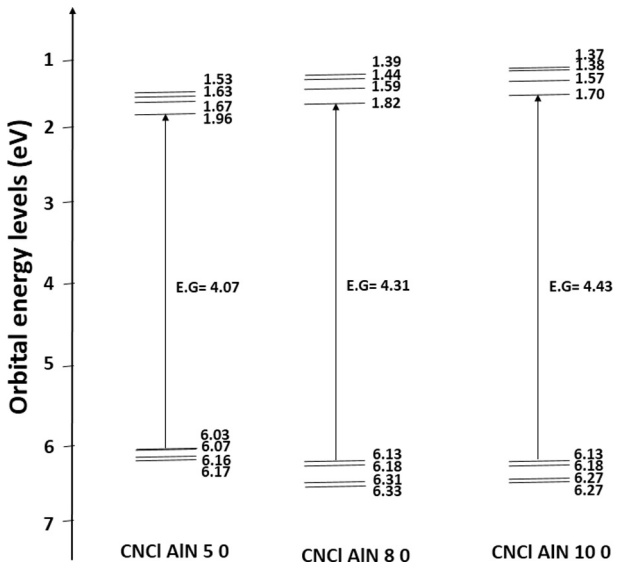

Figure 4 Diagram of molecular orbital levels of the CNCl molecule upon AlN nanotubes.

complex, a little decrease in global hardness after the interaction between two species indicates a less stable, that is, a more reactive, complex [33]. The softness (S) values are changed from 0.24, 0.23, and 0.22 eV for the lone (5, 0), (8, 0), and (10, 0) AlN nanotubes to 0.25, 0.23, and 0.23 eV in the complexes, respectively. The reported chemical potential of the prepared samples is changed from −4.00, −3.98, and −3.92 eV in the pure (5, 0), (8, 0), and (10, 0) AlN nanotubes to −4.27, −4.19, and −4.10 eV after the adsorption process, respectively. As shown in Table 1, the electrophilicity values for whole complexes are decreased. The electrophilicity index is a measure of electrophilic power of a system. Lower electrophilicity index indicates lower electrophilicity of a system [34,35]. Therefore, these results along with the representative energy gap (E_g) values stand for the good condition of (10, 0) AlN for CNCl adsorption.

3.2. TD-DFT calculations

TD-DFT calculations for CNCl molecules that interacted with AlN nanotubes were studied using the B3LYP method and 6-31G** basis set [36]. The details of these calculations are summarized in Table 2. As seen in Table 2, CNCl/(5, 0) AlNNT complex has three excited states in wavelengths of 375.66, 353.53 and 341.83 nm with oscillator strength (f) values of 0.0002, 0.0007 and 0.0002, respectively. The transition from HOMO−1 to LUMO is about 90% that is the main transition. There are two transitions for the CNCl/(8, 0) AlNNT, in wavelengths 327.46 and 323.92 nm with f values of 0.0002 and 0.0003, respectively. Electron transfer occurred from HOMO−1 to LUMO in λ = 275.06 nm, with an amount of 90%. The CNCl/(10, 0) AlNNT complex contains two transitions at 315.12 and 311.01 nm with f values of 0.0001 and 0.0002, respectively. At a wavelength of 311.01 nm, 78% electron transfer occurs from HOMO−1 to LUMO that is the main transition. The UV–Vis absorption spectrum of CNCl reacting with different kinds of AlN nanotubes and with different diameters is shown in Fig. 3. The UV–Vis absorption

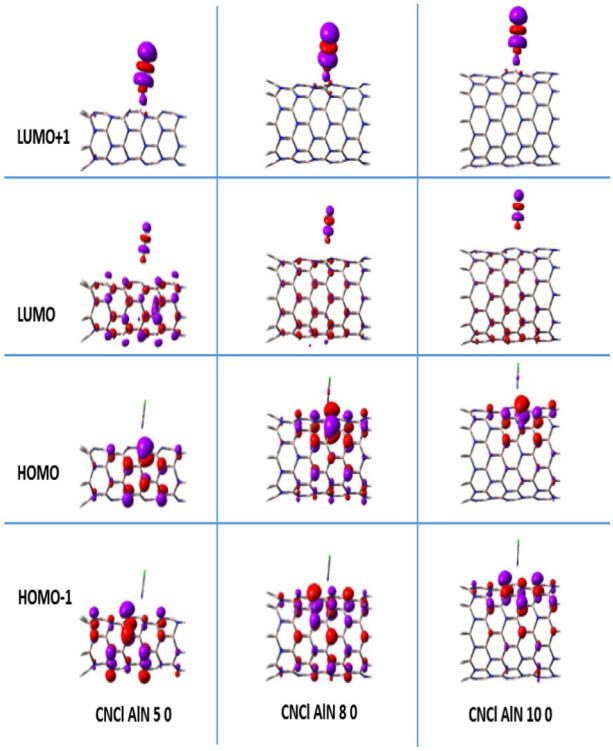

Figure 5 Molecular orbital spatial orientation of the CNCl molecule upon AlN nanotubes.

spectrum of (5, 0) the AlN nanotube exhibits a strong band at 353.53 nm. However, (8, 0) the AlN nanotube shows a band at 323.92 nm and also the UV–Vis absorption spectrum of (10, 0) AlN nanotube exhibits a band at 311.01 nm. Fig. 4 shows the four highest and four lowest molecular orbital energy levels of the CNCl molecule upon AlN nanotubes. Note that the HOMO–LUMO gap of the CNCl/(5, 0) AlN nanotube is relatively smaller than those of the other nanotubes. In addition, the change in energy gap is increased as the AlN nanotubes diameter increases. The HOMO, HOMO−1, LUMO, and LUMO+1 plots for all the applied systems are shown in Fig. 5. The HOMO plot shows that the electron density is localized over the Al atoms of AlNNT while the LUMO plot indicates that the electron density is more localized upon the N atoms of the tube as is also situated on the N–C–Cl bonds of the molecule.

4. Conclusions

The interaction of CNCl toxic molecule over the geometrical structures, energies, electronic properties of various adsorbent kinds containing (5, 0), (8, 0), and (10, 0) AlN nanotubes has been investigated using DFT calculations. The results revealed that the adsorption of CNCl on (5, 0) AlN nanotube is slightly higher than that of (8, 0) and (10, 0) AlN nanotubes. The tubes with larger diameter exhibited better performance in the interaction with CNCl molecule (with a decrease of energy gap) compared to smaller diameter. While the charge transfers from CNCl to AlN nanotube with smaller diameter has better condition than larger diameter. Therefore, our result revealed that the AlN nanotube with smaller diameter would be more effective as adsorbent for the adsorption of the CNCl molecule.

Acknowledgments

We would like to thank the Jaber Ebne Hayyan Unique Industry researchers Company, Gorgan city, Iran. We should also thank the Golestan University of Medical Science, Gorgan, Iran.

References

[1] W. Liu, L.-M. Cheung, X. Yang, C. Shang, THM, HAA and CNCl formation from UV irradiation and chlor(am)ination of selected organic waters, Water Res. 40 (2006) 2033–2043.
[2] X. Yang, C. Shang, Quantification of aqueous cyanogen chloride and cyanogens bromide in environmental samples by MIMS, Water Res. 39 (2005) 1709–1718.
[3] D.W. Kononen, Acute toxicity of cyanogen chloride to *Daphnia magna*, Bull. Environ. Contam. Toxicol. 41 (3) (1988) 371–377.
[4] A. Soltani, M.T. Baei, E. Tazikeh Lemeski, K. Hosseni Amirabadi, Adsorption of cyanogen chloride over Al- and Ga-doped BN nanotubes, Superlattices Microstruct. (2014).
[5] M.T. Baei, A. Ahmadi Peyghan, Z. Bagheri, Covalent functionalization of AlN nanotubes with acetylene, Physica E 47 (2013) 147–151.
[6] J.-M. Zhang, H.-H. Li, Y. Zhang, K.-W. Xu, Structural, electronic and magnetic properties of the 3d transition-metal-doped AlN nanotubes, Physica E 43 (2011) 1249–1254.
[7] S. Hou, J. Zhang, Z. Shen, X. Zhao, Z. Xue, First-principles calculations on the open end of single-walled AlN nanotubes, Physica E 27 (2005) 45–50.
[8] M.T. Baei, A. Ahmadi Peyghan, Z. Bagheri, Fluorination of the exterior surface of AlN nanotube: a DFT study, Superlattices Microstruct. 53 (2013) 9–15.
[9] V.N. Tondare, C. Balasubramanian, S.V. Shende, D.S. Joag, V.P. Godbole, S.V. Bhoraskar, M. Bhadbhade, Field emission from open ended aluminum nitride nanotubes, Appl. Phys. Lett. 80 (2002) 4813–4815.
[10] Q. Wu, Z. Hu, X. Wang, Y. Lu, X. Chen, H. Xu, Y. Chen, Synthesis and characterization of faceted hexagonal aluminum nitride nanotubes, J. Am. Chem. Soc. 125 (34) (2003) 10176–10177.
[11] K. Rezouali, M.A. Belkhir, A. Houari, J. Bai, Ab initio study of confinement and surface effects in hexagonal AlN nanotubes, Comput. Mater. Sci. 45 (2009) 305–309.
[12] D. Zhang, R.Q. Zhang, Theoretical prediction on aluminum nitride nanotubes, Chem. Phys. Lett. 371 (2003) 426–432.
[13] I. Vurgaftman, J.R. Meyer, Band parameters for nitrogen-containing semiconductors, J. Appl. Phys. 94 (6) (2003) 3575.
[14] Z. Mahdavifar, M. Haghbayan, Theoretical investigation of pristine and functionalized AlN and SiC single walled nanotubes as an adsorption candidate for methane, Appl. Surf. Sci. 263 (2012) 553–562.
[15] M. Noei, A. Akbar Salari, N. Ahmadaghaei, Z. Bagheri, A. Ahmadi Peyghan, DFT study of the dissociative adsorption of HF on an AlN nanotube, Competes Rendus Chim. 16 (2013) 985–989.
[16] A. Ahmadi, N.L. Hadipour, M. Kamfiroozi, Z. Bagheri, Theoretical study of aluminum nitride nanotubes for chemical sensing of formaldehyde, Sens. Actuators B 161 (2012) 1025–1029.
[17] M.T. Baei, M. Ramezani Taghartapeh, E. Tazikeh Lemeski, A. Soltani, Computational study of OCN chemisorption over AlN nanostructures, Superlattices Microstruct. 72 (2014) 370–382.
[18] A. Soltani, M. Ramezani Taghartapeh, E. Tazikeh Lemeski, M. Abroudi, H. Mighani, A theoretical study of the adsorption behavior of N_2O on single-walled AlN and AlP nanotubes, Superlattices Microstruct. 58 (2013) 178–190.

[19] A. Soltani, M. Ramezani Taghartapeh, H. Mighani, A.A. Pahlevani, R. Mashkoor, A first-principles study of the SCN chemisorption on the surface of AlN, AlP, and BP nanotubes, Appl. Surf. Sci. 259 (2012) 637–642.
[20] J. Beheshtian, A. Ahmadi Peyghan, Z. Bagheri, A first-principles study of H_2S adsorption and dissociation on the AlN nanotube, Physica E 44 (2012) 1963–1968.
[21] Y. Jiao, A. Du, Z. Zhu, V. Rudolph, S.C. Smith, A density functional theory study of CO_2 and N_2 adsorption on aluminium nitride single walled nanotubes, J. Mater. Chem. 20 (2010) 10426–10430.
[22] W.-G. Liu, G.-H. Chen, X.-H. Huang, D. Wu, Y.-P. Yu, DFT studies on the interaction of an open-ended single-walled aluminum nitride nanotube (AlNNT) with gas molecules, J. Phys. Chem. C 116 (2012) 4957–4964.
[23] M. Schmidt et al, General atomic and molecular electronic structure system, J. Comput. Chem. 14 (1993) 1347–1363.
[24] M.T. Baei, A. Ahmadi Peyghan, Z. Bagheri, Quantum chemical analysis on hydrogenated $Zn_{12}O_{12}$ nanoclusters, Competes Rendus Chim. 16 (2013) 122–128.
[25] M. Mirzaei, A. Seif, N.L. Hadipour, The C-doped zigzag AlN nanotube: a computational NMR study, Chem. Phys. Lett. 461 (2008) 246–248.
[26] Y. Kanani, M.T. Baei, A. Varasteh Moradi, A. Soltani, Adsorption mechanism of single OCN and SCN upon single-walled BP nanotubes, Physica E 59 (2014) 66–74.
[27] M.T. Baei, Y. Kanani, V. Joveini Rezaei, A. Soltani, Adsorption phenomena of gas molecules upon Ga-doped BN nanotubes: a DFT study, Appl. Surf. Sci. 295 (2014) 18–25.
[28] M.T. Baei, M. Ramezani Taghartapeh, E. Tazikeh Lemeski, A. Soltani, A computational study of adenine, uracil, and cytosine adsorption upon AlN and BN nano-cages, Physica B 444 (2014) 6–13.
[29] Nanotube Modeler, JCrystalSoft, 2004–2005. <http://www.jcrystal.com/products/wincnt/>.
[30] Y. Jiao, A. Du, Z. Zhu, V. Rudolphb, S.C. Smith, A density functional theory study of CO_2 and N_2 adsorption on aluminium nitride single walled nanotubes, J. Mater. Chem. 20 (2010) 10426–10430.
[31] S.H. Lim, J. Lin, Ab initio study of the hydrogen chemisorption of single-walled aluminum nitride nanotubes, Chem. Phys. Lett. 466 (2008) 197–204.
[32] J. Beheshtian, M.T. Baei, A. Ahmadi Peyghan, Z. Bagheri, Electronic sensor for sulfide dioxide based on AlN nanotubes: a computational study, J. Mol. Model. 18 (2012) 4745–4750.
[33] N. Saikia, R.C. Deka, Theoretical study on pyrazinamide adsorption onto covalently functionalized (5,5) metallic single-walled carbon nanotube, Chem. Phys. Lett. 500 (2010) 65–70.
[34] B. Stefane, A. Perdih, A. Pevec, T. Solmajer, M. Kocevar, The participation of 2H-pyran-2-ones in [4 + 2] cycloadditions: an experimental and computational study, Eur. J. Org. Chem. (2010) 5870–5883.
[35] S. Armaković, S.J. Armaković, J.P. Šetrajčić, S.K. Jaćimovski, V. Holodkov, Sumanene and its adsorption properties towards CO, CO_2 and NH_3 molecules, J. Mol. Model. 20 (2014) 2170.
[36] H. Ullah, A.-U.-H. Ali-Shah, S. Bilal, K. Ayub, DFT study of polyaniline NH_3, CO_2, and CO gas sensors: comparison with recent experimental data, J. Phys. Chem. C 117 (2013) 23701–23711.